A COMPARISON OF MASS LUMPING TECHNIQUES FOR THE TWO–DIMENSIONAL NAVIER–STOKES EQUATIONS

Dean A. Niclasen
Department of Mechanical Engineering
Monash University
Clayton, Victoria
AUSTRALIA

Hugh M. Blackburn
Division of Building, Construction and Engineering
Commonwealth Scientific and Industrial Research Organisation (CSIRO)
Highett, Victoria
AUSTRALIA

ABSTRACT

The use of finite element spatial approximations to the time–dependent Navier–Stokes equations leads to the solution of one or more matrix–vector systems of linear equations per time step. The solution of some of these systems can be reduced to trivial vector–vector multiplications by reducing system mass matrices to diagonal form, thus achieving significant economies. The sizes of the errors introduced by employing diagonal mass matrices are examined by comparison to an exact solution of the Navier–Stokes equations.

INTRODUCTION

The Galerkin finite element method of discretising the time–dependent Navier–Stokes equations is an attractive method when the solution domain is irregular and cannot be conveniently mapped to a rectangular grid. Generally the method requires the solution of a set of equations of the form

$$[M]\,\dot{\mathbf{u}} = [K]\,\mathbf{u} + \mathbf{f} \tag{1}$$

at each time step. The mass matrix $[M]$ is not diagonal and may lack structure. The cost of solving the resulting system provides an incentive for reducing the consistent mass matrix to diagonal form, thereby reducing the solution procedure in equation (1) to a vector–vector multiplication. Various methods can be used to perform the diagonalisation (Zienkiewicz & Taylor 1991), but all of them incur some numerical error compared to using the consistent mass matrix.

The most common method employed for diagonalisation of $[M]$ is known as row sum lumping, whereby the diagonal term in each row of the lumped matrix is the sum of all of the terms in the row of the consistent matrix:

$$M_{\mathrm{lumped}\,ii} = \sum_{j=1}^{n} M_{\mathrm{consistent}\,ij}. \tag{2}$$

Another means of forming a diagonal mass matrix is to use Gauss–Lobatto–Legendre (GLL) quadrature in the calculation of the mass matrix (see e.g. Hughes 1987). Due to the location of the quadrature points at the element nodes, this integration method automatically generates diagonal element mass matrices.

The effects of mass lumping in finite element discretisations has been studied by Gresho, Lee & Sani (1978), but their study was restricted to advection and advection/diffusion problems, and low element orders. For advection they found that the use of mass lumping in conjunction with 8–noded (serendipity) quadratic elements led to solutions of lower accuracy than the use of the consistent mass matrix in conjunction with 4–noded linear elements. When mass lumping was used with a nine–noded Lagrange quadratic element to solve an advection problem, the accuracy obtained was almost the same as that obtained with linear basis functions using the consistent mass matrix and the same total number of nodes. They did not test the Lagrange quadratic element for solutions of advection–diffusion problems.

In this paper, we examine the loss of solution accuracy associated with mass lumping when applied to a two–dimensional finite element discretisation of the incompressible Navier–Stokes. The effect of mass lumping on solution accuracy is examined for three different element families. Errors are compared with reference to an exact solution of the Navier–Stokes equations. Row–sum lumping and GLL quadrature are compared.

NUMERICAL METHOD

Fractional step method

The time integration scheme used is a fractional step method, which has been widely used with finite difference methods (Chorin 1968) as well as finite element methods (Comini & DelGuidice 1972). The scheme is first order accurate in time. An intermediate velocity field is calculated, without the effect of pressure being applied. The pressure field is then derived from a pressure Poisson equation, and then finally the velocity is updated by applying the new pressure field:

$$\frac{u_i{}^* - u_i{}^{(n)}}{\Delta t} = \left[\nu \frac{\partial^2 u_i{}^{(n)}}{\partial x_j \partial x_j} - \frac{\partial}{\partial x_j}\left(u_i{}^{(n)} u_j{}^{(n)}\right)\right] \quad (3)$$

$$\frac{\partial^2 p^{(n+1)}}{\partial x_i \partial x_i} = \frac{1}{\Delta t}\frac{\partial u_i{}^*}{\partial x_i} \quad (4)$$

$$\frac{u_i{}^{(n+1)} - u_i{}^*}{\Delta t} = -\frac{1}{\rho}\frac{\partial p^{n+1}}{\partial x_i}. \quad (5)$$

Discretisation by the finite element method, using linear, quadratic, or cubic Lagrange elements, leads to the following steps:

$$[M]\frac{\mathbf{u}^* - \mathbf{u}^n}{\Delta t} = [K_1]\mathbf{u}^n \quad (6)$$

$$[H]\mathbf{p} = [K_2]\mathbf{u}^* \quad (7)$$

$$[M]\frac{\mathbf{u}^{n+1} - \mathbf{u}^*}{\Delta t} = [K_3]\mathbf{p}. \quad (8)$$

Lumping $[M]$ to produce a diagonal matrix leads to significant saving of computations in solving equations (6) and (8).

Element Families

Linear-velocity/constant-pressure elements, quadratic-velocity/linear-pressure elements, and cubic-velocity/quadratic-pressure element families were tested. All elements were quadrilaterals of uniform size. The use of lower interpolation order for pressure eliminates the checkerboard pressure mode that can occur when elements with equal interpolation orders are used for both velocity and pressure fields (Sani, Gresho, Lee, Griffiths & Engleman 1981). Figure 1 shows the location of the velocity and pressure nodes for the three element families.

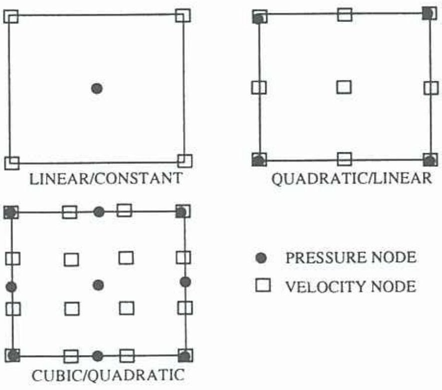

Figure 1: ELEMENT FAMILIES.

TEST PROBLEM

The test problem was an exact solution of the Navier-Stokes equations first published by Taylor (1923) (see also Chorin 1968). The solution domain is the square $-\pi \le x_i \le \pi$, $i = 1, 2$. The boundary conditions are

$$u_1 = -\cos x_1 \sin x_2 \exp(-2t),$$

$$u_2 = -\sin x_1 \cos x_2 \exp(-2t) \quad (9)$$

with initial conditions

$$u_1 = -\cos x_1 \sin x_2, \; u_2 = -\sin x_1 \cos x_2 \quad (10)$$

and an exact solution

$$u_1 = -\cos x_1 \sin x_2 \exp(-2t),$$

$$u_2 = -\sin x_1 \cos x_2 \exp(-2t)$$

$$p = -Re\frac{1}{4}(\cos 2x_1 + \cos 2x_2)\exp(-4t). \quad (11)$$

The Reynolds number (Re) was set to 100 for all the tests presented here. Figure 2 shows pressure contours and velocity vectors/streamlines for the exact solution.

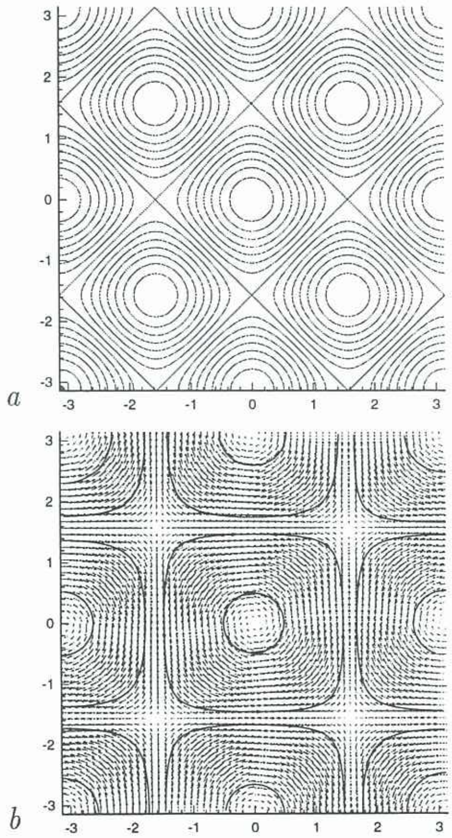

Figure 2: PRESSURE CONTOURS (a) AND VELOCITY VECTOR FIELD AND STREAMLINES (b) FOR THE TEST PROBLEM.

ERROR CALCULATIONS

Numerical values for the L_2 error norm and Sobolev-1 (h_1) error norm for the velocity field were calculated by interpolating the solution onto a fine mesh, and then integrating numerically.

$$L_2{}^2 = \sum^{\text{Elements}} \left[\int_\Omega (u_i - \hat{u_i})(u_i - \hat{u_i})\, d\Omega \right] \quad (12)$$

$$\begin{aligned} h_1{}^2 &= \sum^{\text{Elements}} \left[\int_\Omega (u_i - \hat{u_i})(u_i - \hat{u_i}) \right. \\ &\quad \left. +(u_{i,j} - \hat{u}_{i,j})(u_{i,j} - \hat{u}_{i,j})\, d\Omega \right], \quad (13) \end{aligned}$$

where $\hat{u}$ is the exact solution.

For smooth problems the rate of spatial convergence is given by $O(k+1-m)$, where k is the degree of complete polynomial in the element shape function, and m is 0 for the L_2 norm and 1 for the h_1 norm (Hughes 1987). For example, for quadratic-velocity elements, the expected rate of spatial convergence is $O(3)$ in the L_2 norm and $O(2)$ in the h_1 norm.

CONVERGENCE PROPERTIES FOR QUADRATIC–VELOCITY/LINEAR–PRESSURE ELEMENT

The quadratic-velocity/linear-pressure element family was used for investigation into the spatial convergence properties of the method, with the results presented in Table 1 and Figure 3. In each case, 1000 time steps were used to obtain a solution. A small time step, $\Delta t = 1 \times 10^{-5}$, was chosen to ensure spatial discretisation errors dominated temporal discretisation errors for these tests.

Table 1: MESH RESOLUTION ERRORS FOR QUADRATIC–VELOCITY/LINEAR–PRESSURE ELEMENTS.

Elements	Mass Matrix	L_2	h_1
20 × 20	consistent	1.17×10^{-3}	2.44×10^{-2}
25 × 25	consistent	5.85×10^{-4}	1.52×10^{-2}
30 × 30	consistent	3.34×10^{-4}	1.04×10^{-2}
35 × 35	consistent	2.09×10^{-4}	7.59×10^{-3}
40 × 40	consistent	1.39×10^{-4}	5.78×10^{-3}
20 × 20	row-sum	1.22×10^{-3}	2.48×10^{-2}
25 × 25	row-sum	6.20×10^{-4}	1.56×10^{-2}
30 × 30	row-sum	3.55×10^{-4}	1.07×10^{-2}
35 × 35	row-sum	2.22×10^{-4}	7.78×10^{-3}
40 × 40	row-sum	1.48×10^{-4}	5.90×10^{-3}
20 × 20	Lobatto	1.17×10^{-3}	2.43×10^{-2}
25 × 25	Lobatto	5.91×10^{-4}	1.52×10^{-2}
30 × 30	Lobatto	3.37×10^{-4}	1.04×10^{-2}
35 × 35	Lobatto	2.10×10^{-4}	7.61×10^{-3}
40 × 40	Lobatto	1.40×10^{-4}	5.79×10^{-3}

The results presented in Table 1 and Figure 3 indicate the anticipated rates of spatial convergence were achieved. Mass lumping had no effect on the convergence order and little effect on the magnitude of the errors.

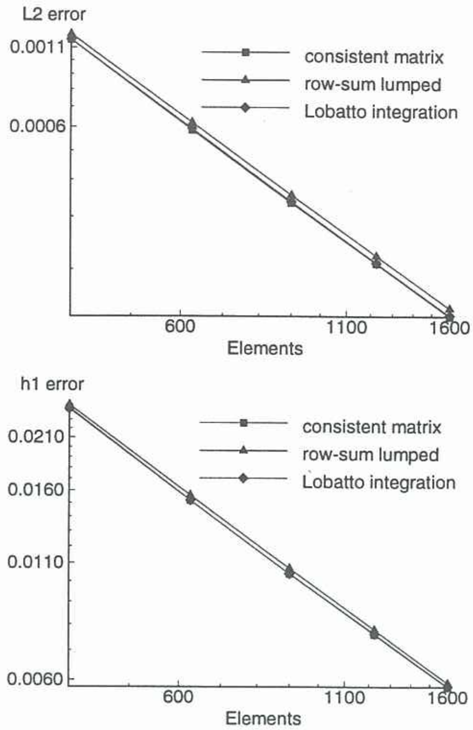

Figure 3: L_2 AND h_1 ERROR NORMS VERSUS NUMBER OF ELEMENTS FOR QUADRATIC–VELOCITY/LINEAR–PRESSURE ELEMENTS.

The error in the L_2 norm for GLL integration was only about 1% greater than that resulting from the consistent mass matrix. This is clearly an acceptable loss in accuracy for many applications, given the substantial savings in computational cost. The use of row-sum lumping lead to an increase typically around 5% over the consistent matrix results. While this is also an acceptable error in most cases, the results for row-sum lumping were always worse than those obtained using GLL integration to obtain a diagonal mass matrix.

The h_1 error norm showed similar behaviour to the L_2 error norm. These results indicate that, for the quadratic-velocity/linear-pressure element family, the use of GLL integration to form a diagonal mass matrix is slightly preferable to applying row-sum lumping to a mass matrix formed using standard Gauss–Legendre integration.

EFFECT OF ELEMENT ORDER ON MASS LUMPING ERROR

The results in the previous section were specific to quadratic-velocity/linear-pressure elements. To examine the relationship between element order and mass lumping, results are compared for the three different element types given in Table 2, with two different mesh sizes also being compared. The coarser mesh had 61 × 61 node points, corresponding to 60 × 60 linear elements, 30 × 30 quadratic elements, and 20 × 20 cubic elements. The finer mesh had 81 × 81 node points, giving 80 × 80 linear elements, 40 × 40 quadratic elements, and 27 × 27 cubic elements. Again, the time step sizes were selected to ensure spatial convergence errors dominated temporal errors.

Table 2: EFFECT OF ELEMENT ORDER ON MASS LUMPING ERRORS

Elements	Mass Matrix	L_2	h_1
Linear–velocity/constant–pressure elements			
60 × 60	consistent	8.64×10^{-3}	1.90×10^{-1}
60 × 60	row-sum	8.62×10^{-3}	1.90×10^{-1}
60 × 60	Lobatto	8.62×10^{-3}	1.90×10^{-1}
80 × 80	consistent	5.03×10^{-3}	1.42×10^{-1}
80 × 80	row-sum	5.02×10^{-3}	1.42×10^{-1}
80 × 80	Lobatto	5.02×10^{-3}	1.42×10^{-1}
Quadratic–velocity/linear–pressure elements			
30 × 30	consistent	3.34×10^{-4}	1.04×10^{-2}
30 × 30	row-sum	3.55×10^{-4}	1.07×10^{-2}
30 × 30	Lobatto	3.37×10^{-4}	1.04×10^{-2}
40 × 40	consistent	1.39×10^{-4}	5.78×10^{-3}
40 × 40	row-sum	1.48×10^{-4}	5.90×10^{-3}
40 × 40	Lobatto	1.40×10^{-4}	5.79×10^{-3}
Cubic–velocity/quadratic–pressure elements			
20 × 20	consistent	6.57×10^{-5}	1.73×10^{-3}
20 × 20	row-sum	6.30×10^{-4}	1.31×10^{-2}
20 × 20	Lobatto	6.71×10^{-4}	1.38×10^{-2}
27 × 27	consistent	2.10×10^{-5}	7.33×10^{-4}
27 × 27	row-sum	2.66×10^{-4}	7.40×10^{-3}
27 × 27	Lobatto	2.82×10^{-4}	7.69×10^{-3}

For each of the element families, the results produced by row–sum lumping and GLL element quadrature in the mass matrix were very similar.

For the linear elements, there was virtually no degradation of the solution accuracy when a diagonal matrix was used. This indicates that mass lumping is a viable option when using linear–velocity/constant–pressure elements for solutions of the Navier–Stokes equations.

The use of a diagonal matrix with the quadratic–velocity elements produced very small degradation in accuracy. As was the case for linear–velocity elements, there was virtually no difference in error levels for the two lumping schemes tested.

The most significant effect of mass lumping was observed for the cubic elements. The use of either form of mass lumping lead to large increases in solution error. The L_2 and h_1 error norms were an order of magnitude higher when either of the diagonal mass matrix schemes were used.

The use of mass lumping schemes with the cubic–velocity/quadratic–pressure elements lead to increased solution errors. This loss of accuracy would be expected to get worse as the element order is increased. For a simple rectangular domain, the cubic–velocity element has a mass matrix bandwidth of 49 for two dimensions, compared to a bandwidth of 25 for the quadratic elements and 9 for the linear elements. As element bandwidth increases, the diagonal form of the assembled matrix will become a poorer approximation of the consistent matrix, and further deterioration in solution accuracy will result. For simple rectangular domains where no more than four elements share the one node–point, the assembled bandwidth is given by $(2 \times N + 1)^2$ where N is the element order. In three dimensions the bandwidth is of order N^3 rather than N^2, hence the effects of using a diagonal mass matrix are expected to be more severe.

CONCLUSIONS

The use of a diagonal mass matrix does not lead to any significant degradation of solution accuracy when used with linear–velocity/constant–pressure or quadratic–velocity/linear–pressure elements in two dimensions. The decrease in computational cost when using the diagonal matrix makes this an attractive choice for unsteady, incompressible Navier–Stokes solvers.

The consistent mass matrix should be used with cubic–velocity/quadratic–pressure elements because diagonal forms of the matrix lead to marked degradation in the solution accuracy.

In all cases tested, there was little observable difference in the levels of additional error produced by either of the two lumping schemes.

REFERENCES

Chorin, A. (1968). Numerical solution of the Navier–Stokes equations, *Math. Comp.* **22**: 742–762.

Comini, G. & DelGuidice, S. (1972). Finite element solution of the incompressible Navier–Stokes equations, *Numerical Heat Transfer* **5**: 463–478.

Gresho, P., Lee, R. & Sani, R. (1978). Advection–dominated flows, with emphasis on the consequences of mass lumping, *Finite Elements in Fluids*, Wiley and Sons, chapter 19.

Hughes, T. J. (1987). *The Finite Element Method*, Prentice–Hall.

Sani, R., Gresho, P., Lee, R., Griffiths, D. & Engleman, M. (1981). The cause and cure (?) of the spurious pressures generated by certain FEM solutions of incompressible Navier–Stokes equations, *Int. J. Num. Meth. Fluids* **1**: 17–43, 171–204.

Taylor, G. (1923). On the decay of vortices in a viscous fluid, *Phil. Mag.* **46**: 671–674.

Zienkiewicz, O. & Taylor, R. (1991). *The Finite Element Method*, 4th edn, McGraw–Hill.